DOI 10.1007/s10778-015-0703-9
International Applied Mechanics, Vol. 51, No. 4, July, 2015

STRESS–STRAIN STATE OF FLEXIBLE ORTHOTROPIC CYLINDRICAL SHELLS WITH A REINFORCED CIRCULAR HOLE

V. A. Maksimyuk[*], E. A. Storozhuk[*], and I. S. Chernyshenko[**]

The stress–strain state of flexible orthotropic cylindrical shells with a reinforced circular hole under static loading is analyzed numerically. The incremental-loading procedure, modified Newton–Kantorovich method, and finite-element method are used. The effect of geometrical nonlinearity, the orthotropy of the material, and the stiffness of the reinforcement in a shell subject to uniform internal pressure on the distribution of stresses, strains, and displacements along the hole edge and in the zone of their concentration is studied

Keywords: flexible orthotropic cylindrical shell, geometrical nonlinearity, stress concentration, reinforced circular hole, finite deflections, internal pressure

Introduction. Traditionally, a shell with a reinforced hole is considered as a structure that consists of the shell proper and a one-dimensional thin rod reinforcing it. The stress–strain state (SSS) of each of these components is described by an applied theory and has its peculiarities. Therefore, the development of a theory that describes the SSS of shells with reinforced holes involves difficulties associated with the necessity of describing the combined action of components with different dimensionality and satisfying the interface conditions [4, 7]. Note that the same difficulties are encountered in studying the SSS of ribbed shells [3, 6, 12, 17].

Most results on stress concentration in isotropic and anisotropic shells with reinforced holes were obtained by solving linear elastic problems with analytic, variational, and numerical methods and are reviewed in [4, 7, 11, 16].

Much fewer studies are concerned with nonlinear boundary-value problems of stress concentration, but mainly for shells of revolution under an axisymmetric load [4, 10, 13].

Very few publications report on solution of nonlinear two-dimensional problems for shells with reinforced holes. For example, the effect of plastic strains and finite deflections on the SSS of isotropic shells with a reinforced curved hole was analyzed in [7, 20]. A nonclassical approach to the design of thin composite shells with reinforced curved holes that employs the same formulas for the shell and the reinforcement was proposed in [14], where some numerical results on the nonlinear deformation of a flexible orthotropic cylindrical shell with a reinforced circular hole under uniform internal pressure are presented.

It is of considerable interest to study the effect of a reinforced hole on the stability of composite shells [9, 18, 19].

In what follows, we will use the approach described in [14] to formulate geometrically nonlinear problems for thin orthotropic cylindrical shells with a reinforced circular hole, outline a numerical method for solving this class of problems, and study the effect of geometrical nonlinearity, the orthotropy of the material, and the stiffness of the reinforcement on the distribution of displacements, strains, and stresses in the zone of their concentration.

1. Problem Formulation. Basic Nonlinear Equations. Consider a thin cylindrical shell of radius R and thickness h_0 made of an orthotropic material and having a circular hole of radius r_0. The shell is described in a curvilinear orthogonal coordinate system (x, y, γ) with the origin at the center of the hole (x, y, and γ are the longitudinal, circumferential, and normal (to

S. P. Timoshenko Institute of Mechanics, National Academy of Sciences of Ukraine, 3 Nesterova St., Kyiv, Ukraine 03057, e-mail: [*]desc@inmech.kiev.ua, [**]prikl@inmech.kiev.ua. Translated from Prikladnaya Mekhanika, Vol. 51, No. 4, pp. 71–80, July–August 2015. Original article submitted December 12, 2013.

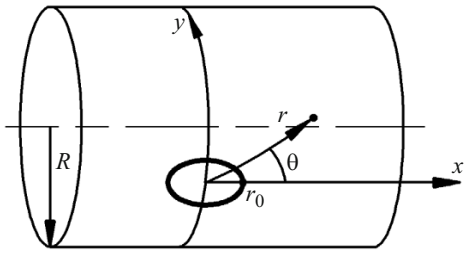

Fig. 1

the coordinate surface) coordinates). The shell is under surface, $\{p\} = \{p_1, p_2, p_3\}^T$, and boundary, $\{m_k\} = \{T_k, S_k, Q_k, M_k\}^T$, forces. Let the midsurface (Σ_0) be a coordinate surface (reference surface $\gamma = 0$). On the developed coordinate surface, we introduce a polar coordinate system (r, θ) (Fig. 1) with one coordinate line ($r = r_0$) coinciding with the boundary of the hole.

Let the hole be reinforced with a curved rod. The reinforcement is modeled by a fragment of a cylindrical shell whose midsurface is equidistant from the midsurface of the shell. Let the equidistant surface (Σ_1) that is in contact with the midsurface of the shell be the coordinate surface. This makes it possible to use the same equations to model both the shell and the curved rod and to describe the behavior of the latter in tension (compression), torsion, and bending in two planes. Such an approach to the design of ribbed shells was proposed in [1] in the late 1960s. Later, a similar approach was used to develop a geometrically nonlinear theory of shallow and deep shells of discretely variable thickness [2, 3].

High loads cause large (finite) deflections in the elastic shell and the reinforcement. To describe the deformation of such a shell and a thin reinforcement rod, we will use the second-order geometrically nonlinear theory of deep shells based on the Kirchhoff–Love hypotheses [4].

The membrane (ε_{ij}) and bending (μ_{ij}) strains have the following vector expressions [14]:

$$\varepsilon_{xx} = \varepsilon^0_{xx} + \varepsilon^*_{xx}, \quad \varepsilon^0_{xx} = \vec{e}_x \cdot \frac{\partial \vec{u}}{\partial x}, \quad \varepsilon^*_{xx} = \frac{1}{2}\varphi_x^2,$$

$$\varepsilon_{xy} = \varepsilon^0_{xy} + \varepsilon^*_{xy}, \quad \varepsilon^0_{xy} = \vec{e}_y \cdot \frac{\partial \vec{u}}{\partial x} + \vec{e}_x \cdot \frac{\partial \vec{u}}{\partial y}, \quad \varepsilon^*_{xy} = \varphi_x \varphi_y,$$

$$\mu_{xx} = \mu^0_{xx} = -\vec{e}_x \cdot \frac{\partial \vec{\varphi}}{\partial x}, \quad 2\mu_{xy} = 2\mu^0_{xy} = -\vec{e}_y \cdot \frac{\partial \vec{\varphi}}{\partial x} - \vec{e}_x \cdot \frac{\partial \vec{\varphi}}{\partial y}, \quad \varphi_x = \vec{n} \cdot \frac{\partial \vec{u}}{\partial x},$$

$$e_{xx} = \varepsilon_{xx} + \gamma\mu_{xx}, \quad e_{xy} = \varepsilon_{xy} + 2\gamma\mu_{xy} \quad (x \to y), \tag{1}$$

where $\vec{u} = u\vec{e}_x + v\vec{e}_y + w\vec{n}$ is the displacement vector of particles of the coordinate surface of the shell (reinforcement); $\vec{e}_x$, $\vec{e}_y$, $\vec{n}$ are the unit vectors of the curvilinear orthogonal coordinate system (x, y, γ); $\vec{\varphi} = \varphi_x\vec{e}_x + \varphi_y\vec{e}_y$ is the vector of angles of tangents to the coordinate lines; the superscripts "0" and "*" refer to the linear and nonlinear components of strains.

Let the axes of orthotropy of the material at each point of the shell (reinforcement) coincide with the coordinate axes (x, y, γ); then the constitutive equations have the form of Hooke's law (the coordinate surface being arbitrary):

$$T_{xx} = T^0_{xx} + T^*_{xx}, \quad T_{yy} = T^0_{yy} + T^*_{yy}, \quad T_{xy} = T^0_{xy} + T^*_{xy},$$

$$T^0_{xx} = C_{11}\varepsilon^0_{xx} + C_{12}\varepsilon^0_{yy} + K_{11}\mu^0_{xx} + K_{12}\mu^0_{yy},$$

$$T^0_{yy} = C_{21}\varepsilon^0_{xx} + C_{22}\varepsilon^0_{yy} + K_{21}\mu^0_{xx} + K_{22}\mu^0_{yy}, \quad T^0_{xy} = C_{33}\varepsilon^0_{xy} + K_{33}2\mu^0_{xy},$$

$$T^*_{xx} = C_{11}\varepsilon^*_{xx} + C_{12}\varepsilon^*_{yy}, \quad T^*_{yy} = C_{21}\varepsilon^*_{xx} + C_{22}\varepsilon^*_{yy}, \quad T^*_{xy} = C_{33}\varepsilon^*_{xy},$$

$$M_{xx} = M^0_{xx} + M^*_{xx}, \quad M_{yy} = M^0_{yy} + M^*_{yy}, \quad M_{xy} = M^0_{xy} + M^*_{xy},$$

$$M_{xx}^0 = K_{11}\varepsilon_{xx}^0 + K_{12}\varepsilon_{yy}^0 + D_{11}\mu_{xx}^0 + D_{12}\mu_{yy}^0,$$

$$M_{yy}^0 = K_{21}\varepsilon_{xx}^0 + K_{22}\varepsilon_{yy}^0 + D_{21}\mu_{xx}^0 + D_{22}\mu_{yy}^0, \quad M_{xy}^0 = K_{33}\varepsilon_{xy}^0 + D_{33}2\mu_{xy}^0,$$

$$M_{xx}^* = K_{11}\varepsilon_{xx}^* + K_{12}\varepsilon_{yy}^*, \quad M_{yy}^* = K_{21}\varepsilon_{xx}^* + K_{22}\varepsilon_{yy}^*, \quad M_{xy}^* = K_{33}\varepsilon_{xy}^*, \tag{2}$$

where C_{mn}, K_{mn}, D_{mn} $(m,n = 1,2,\ m = n = 3)$ are the stiffnesses of the shell (reinforcement),

$$C_{mn} = B_{mn}h, \quad K_{mn} = B_{mn}eh, \quad D_{mn} = B_{mn}\left(\frac{h^3}{12} + he^2\right),$$

$$B_{11} = \frac{E_{xx}}{1-\nu_{xy}\nu_{yx}}, \quad B_{22} = \frac{E_{yy}}{1-\nu_{xy}\nu_{yx}}, \quad B_{12} = B_{21} = \nu_{yx}B_{11} = \nu_{xy}B_{22}, \quad B_{33} = G_{xy}, \tag{3}$$

where E_{xx} and E_{yy} are the longitudinal and circumferential elastic moduli, respectively; G_{xy} is the shear modulus in a plane parallel to the coordinate surface; h is the thickness of the shell or the height of the reinforcement; e is the deflection of the midsurface from the coordinate surface.

2. A Method for Solving Geometrically Nonlinear Problems for Orthotropic Cylindrical Shells with a Reinforced Hole. The system of governing equations can be derived using the principle of virtual displacements, modified Newton–Kantorovich method, and finite-element method (FEM) [7]. The total energy of a flexible cylindrical shell with a reinforced hole is given by

$$\Pi^l = \frac{1}{2}\sum_{i=0,1}\iint\limits_{(\Sigma_i)}(\{\Delta\vartheta^l\}^T[D]\{\Delta\vartheta^l\} + \{\Delta\varphi\}^T[\bar{S}]\{\Delta\varphi\})d\Sigma$$

$$+\sum_{i=0,1}\iint\limits_{(\Sigma_i)}(\{\Delta\vartheta^l\}^T\{\Delta m^*\} + \{\Delta\varphi\}^T[\Delta A_L]^T\{\Delta T\})d\Sigma$$

$$-\iint\limits_{(\Sigma_p)}\{\Delta u_0\}^T\{\Delta p\}d\Sigma - \int\limits_{(\Gamma_k)}\{\Delta u_k\}^T\{\Delta m_k\}ds$$

$$+\sum_{i=0,1}\iint\limits_{(\Sigma_i)}\{\Delta\vartheta^l\}^T\{\bar{m}\}d\Sigma - \iint\limits_{(\Sigma_p)}\{\Delta u_0\}^T\{\bar{p}\}d\Sigma - \int\limits_{(\Gamma_k)}\{\Delta u_k\}^T\{\bar{m}_k\}ds, \tag{4}$$

where $\{u_0\} = \{u,v,w\}^T$ and $\{u_k\} = \{u_m, u_\tau, w, -\varphi_m\}^T$ are the displacement vectors of the shell's midsurface and boundary; $\{\vartheta\} = \{\varepsilon_{11}, \varepsilon_{22}, \varepsilon_{12}, \mu_{11}, \mu_{22}, 2\mu_{12}\}^T$ is the strain vector; $\{m\} = \{T_{11}, T_{22}, T_{12}, M_{11}, M_{22}, M_{12}\}^T$ is the vector of internal forces and moments; (Σ_p) is the portion of the domain (Σ_0) on which surface forces are set; (Γ_k) is the portion of the boundary of the midsurface on which boundary forces are set; Δf and $\bar{f}$ denote the increment of the function f over the nth step of loading and its value at the end of the previous step, respectively; $\{\Delta\vartheta^l\}$ are the components of strain increments linear with respect to the increments of the components of the vectors of displacements and rotation angles; $[\bar{S}]$ is the symmetric matrix of accumulated tangential forces; $\{\Delta T\}$ are the increments of the components of the vector of internal forces; $[\Delta A_L]$ and $\{\Delta\varphi\}$ are the matrix and vector of increments of rotation angles; $[D]$ is the stiffness matrix of the shell (reinforcement).

At each iteration of the modified Newton–Kantorovich method, the problem is solved with an FEM in which the vector of angles $\vec{\varphi}$ of tangents to the coordinate lines is not determined by formulas (1), as is the case with the classical FEM for thin shells, but is approximated by biquadratic serendipity polynomials, with the Kirchhoff–Love hypotheses satisfied only at the nodes of finite elements [7].

Such an approach to determining the vector of rotation angles, in essence, implements the Kirchhoff–Love hypotheses in discrete form. The method of discretizing the Kirchhoff–Love hypotheses was first proposed in [8] and was then widely used in designing thin plates and shells [5, 7, 15].

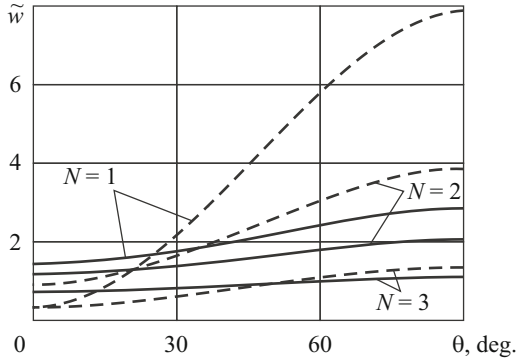

Fig. 2

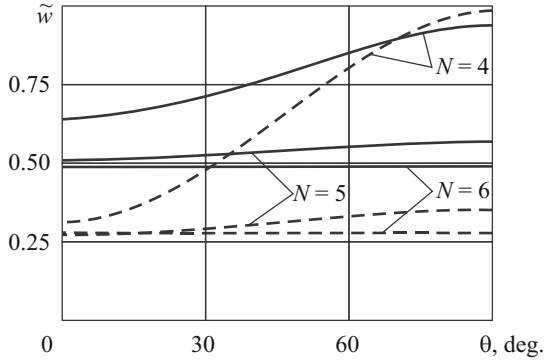

Fig. 3

Using the stationarity conditions for the discrete analog of functional (4) and allowing for finite deflections, we arrive at a system of governing equations for a thin cylindrical composite shell with a reinforced hole, which has the following matrix form at the nth step of loading:

$$\left([K_0]+[K_\varphi]+[K_\sigma]\right)\{\Delta q\}=\{\Delta P\}-\{\Delta\Omega\}+\{\Delta\Psi\}, \tag{5}$$

where $[K_0]$ is the stiffness matrix of the linear elastic shell and reinforcement; $[K_\varphi]$ and $[K_\sigma]$ are the influence matrices of initial angles and stresses; $\{\Delta q\}$ is the vector of increments of nodal degrees of freedom; $\{\Delta P\}$ is the load vector; $\{\Delta\Omega\}$ is the vector of nonlinearities; $\{\Delta\Psi\}$ is the vector of residuals of the equilibrium equations at the end of the $(n-1)$th step of loading.

3. Nonlinear Deformation of a Cylindrical Shell with a Circular Hole Reinforced with a Ring with Varying Stiffness. Let us analyze the effect of the elastic modulus of the reinforcement material on the SSS around a circular hole in a flexible orthotropic organic-plastic cylindrical shell.

The shell has the following characteristics:

$$R/h_0=400,\quad r_0/h_0=30,\quad E_{xx}=25.3\text{ GPa},\ E_{yy}=38.4\text{ GPa},\ G_{xy}=7.6\text{ GPa},\ \nu_{yx}=0.238. \tag{6}$$

The hole is reinforced with a ring of rectangular cross-section of height $h_r=3h_0$, width $b_r=3h_0$, and eccentricity $e_r=0$. The ring is made of a homogeneous isotropic material with Poisson's ratio $\nu^r=0.3$.

The shell is subject to internal pressure $q=q_0\cdot10^5$ Pa, axial tensile forces $T_k=qR/2$ at the ends, and shearing force $Q_k=qr_0^2/(2r_0-b_c)$ applied to the reinforcement axis.

For reasons of geometrical and mechanical symmetry, we can consider a quarter the shell. Symmetry conditions are specified on the lines $x=0$ and $y=0$, boundary conditions are specified at the interface between the shell and the reinforcement, and the stress state far from the hole ($x=6r_0$ and $y=6r_0$) is assumed membrane.

The tables and figures below present the solutions (distribution of displacements, strains, and stresses) of the linear (LP) and geometrically nonlinear (GNP) problems for cylindrical shells with a reinforced circular hole under internal pressure $q_0=2$ for the following Young's moduli of the reinforcement material: (1) $E^r=0$ (N = 1; free hole), (2) $E^r=10$ GPa (N = 2; reinforcement of low stiffness), (3) $E^r=67$ GPa (N = 3; AMg-6 alloy), (4) $E^r=110$ GPa (N = 4; nearly optimal reinforcement), (5) $E^r=10^3$ GPa (N = 5; reinforcement of high stiffness), (6) $E^r=67\cdot10^5$ GPa (N = 6; rigid inclusion).

Figures 2 (N = 1, 2, 3) and 3 (N = 4, 5, 6) shows the variation in the relative deflection $\tilde{w}=w/h_0$ along the boundary of the hole. The dashed and solid lines represent the LP and GNP, respectively.

It can be seen that the deflection is maximum at the point $\theta=90°$ on the boundary of the free hole (N = 1) or the hole with reinforcement of low or moderate stiffness (N = 2, 3, 4) and in the section $\theta=90°$ at a great distance ($r\approx4r_0$ for the LP and $r\approx6r_0$ for the GNP) from the hole with reinforcement of high stiffness or a rigid inclusion (N = 5, 6). Reinforcing the hole with a rod of certain stiffness decreases the maximum deflection. The rigid inclusion reduces the maximum deflection on the hole boundary maximally (by 96% and 83% for the LP and GNP, respectively). As the stiffness of the reinforcement is increased, the maximum deflection monotonically decreases. Allowing for geometrical nonlinearity decreases the maximum deflection in the first four

TABLE 1

Problem	θ	$\tilde{\gamma}$	$e_r \cdot 10^2$					
			$N = 1$	$N = 2$	$N = 3$	$N = 4$	$N = 5$	$N = 6$
LP	0°	0.5	–0.2331	–0.4048	0.0505	0.1064	0.1468	0.0042
		–0.5	–0.4895	0.1893	0.3503	0.3999	0.5075	0.4273
	45°	0.5	–0.7507	–0.1607	0.1742	0.1993	0.2065	0.1277
		–0.5	–0.2818	–0.3055	–0.0575	0.0343	0.2734	0.4195
	90°	0.5	–0.1930	0.1755	0.1358	0.1093	0.0790	0.2300
		–0.5	0.2023	–0.1912	–0.0080	0.0667	0.2328	0.2549
GNP	0°	0.5	–0.2609	–0.2108	0.0898	0.1355	0.1959	0.0470
		–0.5	–0.2582	0.0357	0.2773	0.3487	0.4796	0.4115
	45°	0.5	–0.4321	–0.1570	0.1557	0.1994	0.2471	0.1930
		–0.5	–0.2876	–0.2126	–0.0370	0.0358	0.2554	0.3823
	90°	0.5	–0.1145	0.0329	0.1297	0.1404	0.1475	0.2688
		–0.5	–0.0090	–0.0661	–0.0025	0.0375	0.1770	0.2425

TABLE 2

Problem	θ	$\tilde{\gamma}$	$e_\theta \cdot 10^2$					
			$N = 1$	$N = 2$	$N = 3$	$N = 4$	$N = 5$	$N = 6$
LP	0°	0.5	0.9249	0.8765	0.2409	0.1485	–0.0017	0.0001
		–0.5	2.0691	1.0793	0.3632	0.2390	0.0113	0.0001
	45°	0.5	1.4289	0.7852	0.2448	0.1647	0.0219	0.0001
		–0.5	0.9888	0.5671	0.2360	0.1675	0.0248	0.0001
	90°	0.5	1.2440	0.6237	0.2679	0.1954	0.0458	0.0000
		–0.5	–1.3152	–0.1814	0.0904	0.0867	0.0357	0.0000
GNP	0°	0.5	1.0578	0.7769	0.2721	0.1758	0.0014	0.0002
		–0.5	1.0709	0.7495	0.3037	0.2081	0.0114	0.0002
	45°	0.5	0.9446	0.6104	0.2360	0.1653	0.0235	0.0001
		–0.5	0.7272	0.4961	0.2250	0.1632	0.0255	0.0001
	90°	0.5	0.6992	0.4435	0.2201	0.1685	0.0450	0.0000
		–0.5	0.0315	0.1111	0.1309	0.1093	0.0363	0.0000

cases of reinforcement and increases the maximum deflection on the hole boundary in the fifth and sixth cases. It can be seen that nonlinearity has the strongest effect on the maximum deflection of the shells with free and weakly reinforced holes and the weakest effect in the fourth case of reinforcement. For example, in these cases, the maximum deflections in the GNP differ from those in the LP by 64%, 47%, and 5%, respectively.

Tables 1 and 2 collect the values of the radial (e_r) and circumferential (e_θ) strains at several nodal points ($\theta = 0°$, 45°, 90°) on the hole boundary on the outside ($\tilde{\gamma} = \gamma / h_0 = 0.5$) and inside ($\tilde{\gamma} = -0.5$) surfaces of the shell.

The maximum magnitudes are achieved by the circumferential strains at the point $\theta = 0°$ on the boundary of the hole with no reinforcement ($N = 1$), reinforcement of low stiffness ($N = 2$), and reinforcement made of AMg-6 alloy ($N = 3$) and by the radial strains at the same nodal point $\theta = 0°$ on the inside surface of the shell with more stiffer reinforcement ($N = 4, 5, 6$). As the stiffness of the reinforcement is increased, the maximum strains change nonmonotonically: first they considerably decrease, then slightly increase, and, finally, slightly decrease. The maximum decrease (by 82 and 72% for the LP and GNP, respectively) in the maximum strains is caused by the reinforcement made of AMg-6 alloy. Allowing for finite deflections decreases the maximum strains in all cases of reinforcement. The stiffer the reinforcement, the weaker the effect of geometrical nonlinearity on the maximum strains. For example, the difference between the maximum strains obtained by solving the LP and GNP is 48% for the free hole, 16% for AMg-6 reinforcement, and 3.5% for the rigid inclusion.

The values of the radial ($\sigma_r = \sigma_r^0 \cdot 10^5$ Pa) and circumferential ($\sigma_\theta = \sigma_\theta^0 \cdot 10^5$ Pa) stresses calculated at the same points as the respective strains are summarized in Tables 3 and 4.

The solutions of the LP and GNP suggest that the maximum stresses are observed at the point $\theta = 0°$ of the hole boundary on the inside surface of the shell in all cases of reinforcement. The exception is the rigid inclusion because it makes the stresses in the LP reach their maximum at the point ($r = r_0$, $\theta = 45°$) on the inside surface. The maximum magnitudes are achieved by the circumferential stresses in the shells with no, low-stiffness, and moderate-stiffness reinforcement and by the radial stresses in the shells with high-stiffness reinforcement and rigid inclusion. As the stiffness of the reinforcement is increased, the maximum stresses change nonmonotonically.

Let us identify the optimal reinforcement using a minimax criterion to minimize the maximum stress:

$$N_{\text{opt}} = \arg \min_{N \in [N]} \max_{(x, y, \gamma) \in \Omega} \sigma\left[N, (x, y, \gamma)\right], \tag{7}$$

where $[N]$ is a set of feasible stiffnesses of the reinforcement rod; Ω is the range of variation in the curvilinear coordinates (x, y, γ).

Applying the minimax criterion (7), we reveal that the optimal reinforcement is the rigid inclusion in the LP and the fourth case of reinforcement in the GNP.

Thus, the optimal reinforcement of the hole causes the maximum decrease in the maximum stresses (by 74 and 85% in the GNP and LP, respectively).

Note that for a spherical shell with a reinforced circular hole under uniform internal pressure, the minimax criterion (7) requires the maximum radial and circumferential stresses to be equal ($\sigma_r^{\max} = \sigma_\theta^{\max}$).

Allowing for finite deflections decreases the maximum stresses in all cases of reinforcement. Geometrical nonlinearity manifests itself when the hole is not reinforced or reinforced with a ring of low stiffness. The higher the stiffness of the reinforcement, the weaker its effect on the stress state of the shells. For example, allowing for finite deflections reduces the maximum stresses by 48% in the case of no reinforcement, by 17% in the case of reinforcement made of AMg-6 alloy, and by 7.5% in the case of rigid inclusion.

4. Effect of the Orthotropy of the Material on the Nonlinear Deformation of a Cylindrical Shell with a Reinforced Hole. By changing the orientation of the axes of orthotropy of composites relative to the midsurface coordinate system (x, y), we can analyze the effect of orthotropy on the SSS of shells. Let us compare the SSS of a cylindrical shell made of a material with $\tilde{E} = E_{xx} / E_{yy} = 0.659$ (Sec. 3) and the SSS of the same shell but with a different orientation of the axes of orthotropy such that $\tilde{E} = 1.518$.

Table 5 compares the maximum deflections, strains, and stresses for shells with free ($N = 1$) and reinforced ($N = 3$) holes and with a rigid inclusion ($N = 6$).

The table indicates that as the elastic modulus is increased in the longitudinal direction, the maximum deflections increase by 3, 25, and 54% in the LP and by 16, 34, and 59% in the GNP. It can be seen that in the GNP, the orthotropy of the material has a stronger effect on the deflections than in the LP. The maximum strains increase by 21, 8, and 19% in LP and by 26,

TABLE 3

Problem	θ	$\tilde{\gamma}$	σ_r^0					
			$N = 1$	$N = 2$	$N = 3$	$N = 4$	$N = 5$	$N = 6$
LP	0°	0.5	–33	–515	283	373	385	11
		–0.5	9	1173	1148	1201	1341	1123
	45°	0.5	–7	556	848	824	668	381
		–0.5	–11	–128	222	390	853	1170
	90°	0.5	10	1091	710	558	344	918
		–0.5	–17	–877	25	320	951	1017
GNP	0°	0.5	–23	–67	406	466	516	123
		–0.5	–8	563	919	1047	1268	1082
	45°	0.5	–17	329	778	819	779	560
		–0.5	–10	24	241	371	802	1071
	90°	0.5	–18	409	655	666	617	1072
		–0.5	–19	–194	719	218	729	968

TABLE 4

Problem	θ	$\tilde{\gamma}$	σ_θ^0					
			$N = 1$	$N = 2$	$N = 3$	$N = 4$	$N = 5$	$N = 6$
LP	0°	0.5	3544	3243	993	659	85	3
		–0.5	7949	4422	1668	1204	363	268
	45°	0.5	3306	1994	955	771	387	187
		–0.5	1921	1199	668	592	475	533
	90°	0.5	3150	1749	789	582	170	144
		–0.5	–3330	–597	233	270	240	160
GNP	0°	0.5	4059	2967	1142	786	128	30
		–0.5	4109	3012	1385	1048	346	258
	45°	0.5	2075	1495	900	767	440	267
		–0.5	1533	1101	639	565	453	490
	90°	0.5	932	1186	660	531	211	168
		–0.5	1766	251	343	311	206	152

TABLE 5

$\widetilde{E}$	N	LP			GNP		
		$\widetilde{w}_{\max}$	$e_{\max}\cdot 10^2$	$\sigma^0_{\max}$	$\widetilde{w}_{\max}$	$e_{\max}\cdot 10^2$	$\sigma^0_{\max}$
0.659	1	7.897	2.0691	7949	2.858	1.0709	4109
	3	1.354	0.3632	1668	1.119	0.3037	1385
	6	0.792	0.4273	1170	0.734	0.4115	1082
1.518	1	8.109	2.4971	6317	3.318	1.3429	3396
	3	1.690	0.3915	1295	1.500	0.3336	1069
	6	1.220	0.5098	1374	1.166	0.4615	1320

10, and 12% in the GNP. The effect of orthotropy on the stress state depends on the stiffness of the reinforcement and is opposite in two limiting cases: free hole and rigid inclusion. For example, the maximum stresses in the shells with free and reinforced holes decrease by 21 and 22% in the LP and by 17 and 23% in the GNP, and the maximum stress in the shell with a rigid inclusion increases by 17% in the LP and by 22% in the GNP, which is due to the stronger reinforcing effect of the stiffer portion of the shell on its less stiff portion.

Conclusions. We have formulated geometrically nonlinear problems for thin orthotropic cylindrical shells with a reinforced curved hole and outlined a numerical method for solving them based on the incremental-loading procedure, a modified Newton–Kantorovich method, and the finite-element method. A distinguishing feature of the method is that the same equations are used to describe the deformation of both the shell and the reinforcement and that the Kirchhoff–Love hypotheses used have discrete form. The method and associated software have been used to analyze the effect of finite deflections, orthotropy, and the stiffness of reinforcement on the stress–strain state of a cylindrical shell with a reinforced circular hole under uniform internal pressure. The numerical results have been presented as tables and graphs and analyzed.

REFERENCES

1. P. A. Zhilin, "General theory of ribbed shells," in: *Strength of Hydraulic Turbines* [in Russian], Issue 88, Tr. TsKTI, Leningrad (1968), pp. 46–70.
2. V. V. Karpov, *Models and Algorithms for the Strength and Stability Analyses of Reinforced Shells of Revolution*, Part 1 of *Strength and Stability of Reinforced Shells of Revolution* [in Russian], Fizmatlit, Moscow (2010).
3. V. V. Karpov and A. A. Semenov, "Mathematical model of the deformation of reinforced orthotropic shells of revolution," *Inzh.-Stroit. Zh.*, No. 5, 100–106 (2013).
4. A. N. Guz, I. S. Chernyshenko, V. N. Chekhov, et al., *Theory of Thin Shells Weakened by Holes*, Vol. 1 of the five-volume series *Methods of Shell Design* [in Russian], Naukova Dumka, Kyiv (1980).
5. P. M. A. Areias, J.-H. Song, and T. Belytschko, "A finite-strain quadrilateral shell element based on discrete Kirchhoff–Love constraints," *Int. J. Numer. Meth. Eng.*, **64**, 1166–1206 (2005).
6. D. Bushnell, "Analysis of ring-stiffened shells of revolution under combined thermal and mechanical loading," *AIAA J.*, **9**, No. 3, 401–410 (1971).
7. A. N. Guz, E. A. Storozhuk, and I. S. Chernyshenko, "Nonlinear two-dimensional static problems for thin shells with reinforced curvilinear holes," *Int. Appl. Mech.*, **45**, No. 12, 1269–1300 (2009).
8. L. R. Herrmann and D. M. Campbell, "A finite-element analysis for thin shells," *AIAA J.*, No. 6, 1842–1847 (1968).

9. M. W. Hilburger and J. H. Starnes, “Buckling behavior of compression-loaded composite cylindrical shells with reinforced cutouts,” *Int. J. Non-Linear Mech.*, **40**, No. 7, 1005–1021 (2005).
10. A. Kaufman and D. Spera, “Investigation of the elastic-plastic stress state around reinforced opening in a spherical shell,” *NASA Sci. Tech. Publ.*, Washington (1965).
11. A. Kharat and V. V. Kulkarni, “Stress concentration at openings in pressure vessels – A review,” *Int. J. Innov. Res. Sci.*, *Eng. Tech.*, **2**, No. 3, 670–678 (2013).
12. N. V. Maiborodina and V. F. Meish, “Forced vibrations of ellipsoidal shells reinforced with transverse ribs under a nonstationary distributed load,” *Int. Appl. Mech.*, **49**, No. 6, 693–701 (2013).
13. V. A. Maximyuk, E. A. Storozhuk, and I. S. Chernyshenko, “Nonlinear deformation of thin isotropic and orthotropic shells of revolution with reinforced holes and rigid inclusions,” *Int. Appl. Mech.*, **49**, No. 6, 685–692 (2013).
14. V. A. Maximyuk, E. A. Storozhuk, and I. S. Chernyshenko, “Stress state of flexible composite shells with stiffened holes,” *Int. Appl. Mech.*, **50**, No. 5, 558–565 (2014).
15. S. S. Murthy and R. H. Gallagher, “Anisotropic cylindrical shell element based on discrete Kirchhoff theory,” *Int. J. Numer. Meth. Eng.*, **19**, No. 12, 1805–1823 (1983).
16. W. D. Pilkey and D. D. Pilkey, *Peterson’s Stress Concentration Factors*, John Wiley & Sons, New York (2008).
17. M. S. Qatu, E. Asadi, and W. Wang, “Review of recent literature on static analyses of composite shells: 2000–2010,” *Open J. Comp. Mater.*, No. 2, 61–86 (2012).
18. E. Senocak and A. M. Waas, “Optimally reinforced cutouts in laminated circular cylindrical shells,” *Int. J. Mech. Sci.*, **38**, No. 2, 121–140 (1996).
19. S. Shi, Z. Sun, M. Ren, H. Chen, and X. Hu, “Buckling response of advanced grid stiffened carbon-fiber composite cylindrical shells with reinforced cutouts,” *Compos. Part B: Eng.*, **44**, No. 1, 26–33 (2013).
20. E. A. Storozhuk and I. S. Chernyshenko, “Reinforcement of the contour of a hole in an inelastic shell,” *Int. Appl. Mech.*, **24**, No. 11, 1064–1068 (1988).